

Physical Properties of the Superconducting Ta Film Absorber of an X-ray Photon Detector

L. Li, L. Frunzio, C.M. Wilson, and D.E. Prober

Abstract—We have developed single-photon 1-D imaging detectors based on superconducting tunnel junctions. The devices have a Ta film with an Al/AIO_x/Al tunnel junction on each end and a Nb contact in the center. The best energy resolution of this kind of detector is 13 eV for 5.9 keV x-ray photons. Two devices with different lengths: 500 and 1000 μm are measured to study the non-equilibrium quasiparticle dynamics in the superconducting Ta film. The diffusion constant and lifetime of quasiparticles in the Ta films have been derived by fitting the measured current pulses to the model. The comparison of the simulation and measurement results proves that the quasiparticle loss is not primarily due to the Nb ground contact in the center of the Ta absorber, but is due to the uniform non-thermal loss in the Ta film. The Nb ground contact does contribute to the broadening of the energy width in the center of the Ta film.

Index Terms—diffusion constant, imaging, lifetime, single photon detectors, quasiparticle, Ta.

I. INTRODUCTION

SUPERCONDUCTING tunnel junction detectors (STJs) have been studied during the past decade as non-dispersive, single photon spectrometers for the energy range from 1 eV to 10 keV [1-6] because of their predicted high energy resolving power, $E/\Delta E$. The STJ can be used in astronomical observations, material analysis and other spectroscopy applications. The STJ also provides photon timing information with high quantum efficiency.

We have developed Ta-Al-AIO_x-Al tunnel junction detectors for astrophysical application. The device uses a lateral double junction geometry with a Nb contact in the center of the Ta absorber. With this structure 1-D spatial imaging is possible using only two readout channels.

The basic working principle of the STJ detectors is that the absorption of a single x-ray photon breaks Cooper pairs and creates millions of quasiparticles. The intrinsic energy resolution (Full-Width-at-Half-Maximum, FWHM) of the STJ detectors due to the creation statistics of the single-electron excitations is $\Delta E = 2.355 (F\epsilon E)^{1/2}$, where E is the incident photon energy, $\epsilon = 1.74 \Delta$ (2Δ is the energy gap of a superconductor absorber) is the effective energy required to create a single

excitation (quasiparticle) and F is the Fano factor. We assume $F=0.22$ [7]. For the Ta absorber ($\Delta_{\text{Ta}}=700 \mu\text{eV}$) it gives $\Delta E = 2.96 \text{ eV}$ at 5.9 keV. After quasiparticles are created, they diffuse in the Ta absorber. After reaching the Al trap, they scatter down to lower energy levels by emitting phonons and are trapped. After tunneling through the insulator barrier, the quasiparticles will either tunnel back into the trap or diffuse out into the wiring pads leaving the junction region. The sum of the charges collected by the two junctions is proportional to the photon energy and the charge ratio gives us the position information of the photon.

To date the best energy resolution achieved by this kind of detector is 13 eV over a length of 20 μm of the 200 μm long absorber [6,8]. The spatial non-uniformity of the energy resolution along the Ta absorber is found to be due to the Nb contact. Use of a Ta contact, connected to the trap of one Al junction, significantly improves the spatial uniformity of the energy resolution [8]. In the present work we have measured quasiparticle lifetimes in two devices with different absorber lengths (500, 1000 μm). The two devices give us a consistent quasiparticle lifetime and diffusion constant. The quasiparticle lifetime is longer than that found in our previous work [3], where an earlier, short device was measured. We verified in the present work that the quasiparticle loss is due to uniform loss in the Ta absorber instead of a localized loss caused by the Nb contact. This could not be distinguished in the previous work [3] on a device with a 200 μm long Ta absorber, because the quasiparticle loss in the short Ta absorber is too small to distinguish the cause of quasiparticle loss. It is important for us to determine the quasiparticle dynamics inside the Ta absorber, such as the quasiparticle diffusion constant and the lifetime, since the Ta absorber size and response time are critical for

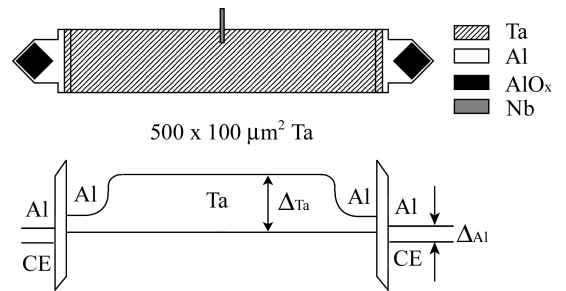


Fig. 1. Geometry of the device with 500 μm long Ta absorber. The black regions are tunnel junctions. A band diagram is also shown (bottom). In the central region, the Fermi level is constant. The counter-electrodes (CE) are noted. The 1000 μm long device has the same junction structure.

Manuscript received August 2, 2002.

Liqun Li, L. Frunzio, C. M. Wilson and D.E. Prober are with the Departments of Applied Physics and Physics, Yale University, New Haven, CT 06520 USA (telephone: 203-432-4280, e-mail: daniel.prober@yale.edu).

potential astronomy applications.

II. DEVICE GEOMETRY AND EXPERIMENTAL SETUP

Two devices of different length were measured in a 2-stage pumped ^3He cryostat at 210 mK. A magnetic field of about 2.5 mT is applied parallel to the substrate to suppress the Josephson current. The device is irradiated with an ^{55}Fe X-ray source which emits MnK_α ($E = 5895$ eV) and MnK_β ($E = 6490$ eV) photons. A low noise current amplifier is used to measure the current signal from each tunnel junction [9]. The two devices have different absorber lengths, 500 μm and 1000 μm , but the same width of 100 μm , and the same junction area, 2025 μm^2 . In the center of the Ta absorber, there is a Nb ground contact, 20 μm long and 5 μm wide. The devices were produced on one passivated Si wafer. The Ta film has residual resistance ratio $\text{RRR}=17$ with $T_c=4.5$ K. The Josephson current density of each device is 30 A/cm^2 . The tunnel time is 3.4 μs . The geometry is shown in Fig. 1. Each device is voltage biased at 130 μV .

III. EXPERIMENTAL RESULTS

Fig. 2 shows the charge outputs Q_1 vs. Q_2 , of the 500 μm long device. Each black dot represents an x-ray photon event. They form two lines in the figure, one is K_α line with less total charge but more events, the other one is K_β line with more total charge but less events. The events which are lower in total charge ($Q_1 + Q_2$) than the K_α line are substrate events. The curvature of Q_1 vs. Q_2 is caused by quasiparticle loss in the Ta absorber. With no quasiparticle loss in the absorber the Q_1 vs. Q_2 plot should be a straight line for a fixed photon energy. If there is quasiparticle

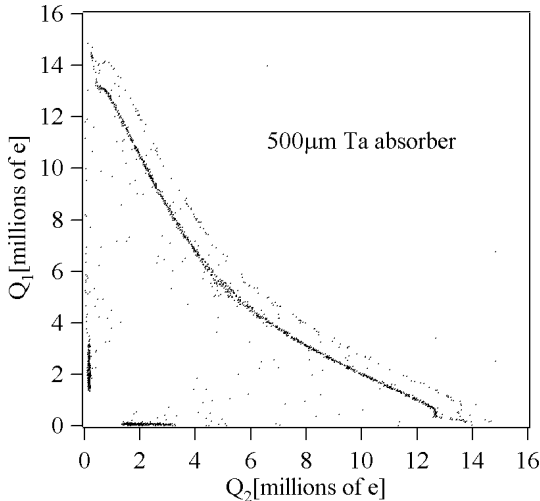


Fig. 2. Q_1 vs. Q_2 plots of the device with a 500 μm long Ta absorber. The dots are measured individual x-ray events. Two main traces are formed by x-ray events from MnK_α and MnK_β photons from an ^{55}Fe source. The events with the energy lower than these two lines are the photons absorbed in the Si substrate. The events at the two ends of the traces are the photons absorbed in the overlap region of Ta absorber and Al junction. Events with Q_1 or $Q_2 = 0$ are due to photons absorbed in the Al wiring.

loss in the Ta absorber, the photon events absorbed in the center suffer more quasiparticle loss than at the edge because it takes a longer time for quasiparticles to diffuse out of the Ta absorber from the center than from the edge. For the 500 μm long device 30% of the quasiparticles generated in the center are lost in the Ta absorber, while 75% of quasiparticles are lost for 1000 μm long device. The pulse times get longer as the absorber length increases, limited by the quasiparticle diffusion constant.

By using two junction detectors, we can implement 1-D imaging and also can study the quasiparticle dynamics, such as the diffusion constant and quasiparticle lifetime, from the measured tunneling current pulse. The quasiparticle lifetime and diffusion constant set the limit for the maximum dimension and response time of the Ta absorber.

IV. SIMULATION

The experimental results show that a significant fraction of the quasiparticles were lost in the two devices. Quasiparticle loss may be caused by spatially uniform loss in the Ta absorber or by loss at the Nb contact in the center, through recombination in the Nb oxide region with a lower energy gap. Nb is used as a ground contact for both tunnel junctions. It has a larger energy gap ($\Delta_{\text{Nb}}=1.4$ meV) than that of Ta, and prevents quasiparticles from diffusing out of the Ta absorber. The fact that the Nb contact causes the energy broadening in the center was proved in previous work [8]. The likely reason is that Nb oxides can be metallic or low-gap superconductors, and trap quasiparticles.

To understand the quasiparticle loss sources, we did numerical simulations to simulate quasiparticle processes in the detectors [10]. In the model used in our simulations, the one-dimensional diffusion equation is used to describe the spatial distribution of the quasiparticle density as a function of time. The diffusion equation for the quasiparticles density $n(x,t)$ in the Ta absorber is

$$\frac{\partial n(x,t)}{\partial t} - D \frac{\partial^2 n(x,t)}{\partial x^2} = -\frac{n(x,t)}{\tau_{\text{Ta}}} - \frac{n(x,t)}{\tau_{\text{Nb}}} \Big|_{x=L/2}, \quad (1)$$

D is the diffusion constant, τ_{Ta} is the quasiparticle lifetime in the Ta and τ_{Nb} the lifetime in the Ta under the Nb contact. The Nb contact overlaps the Ta absorber on one edge, but we treat this as a one-dimensional problem along the length of the absorber as a first approximation.

Fig. 3 shows the simulation results of Q_1 vs. Q_2 with quasiparticle loss from uniform loss in the Ta absorber and from loss due to the Nb contact. If the quasiparticle loss is uniform in the Ta absorber, Q_1 vs. Q_2 is a smooth curve. If the quasiparticles are lost in the Nb contact region, the curve has a pointlike structure in the center of the Q_1 vs. Q_2 plot, and a straight line from the center to the edge. Comparing with the experimental data shown in Fig. 2, we can determine the loss is mainly from the uniform loss in the Ta absorber. The curvature of Q_1 vs. Q_2 can be described by the loss parameter $\alpha=L/(D\tau_{\text{Ta}})^{1/2}$. Since both devices are from the same chip, their

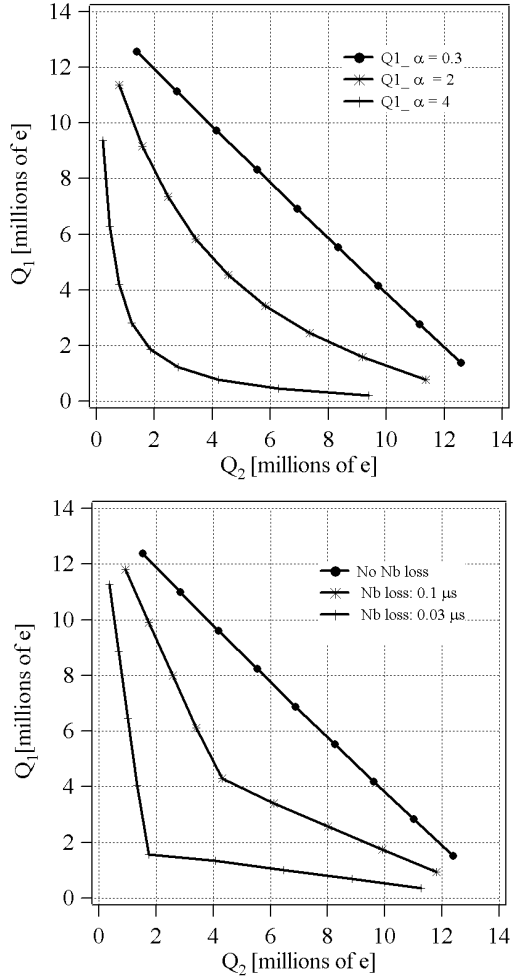


Fig. 3. (a). Q_1 vs. Q_2 with only uniform loss in Ta absorber. (b). Q_1 vs. Q_2 with loss only in the Nb overlap region.

Ta absorbers have the same quality. By fitting the experimental data, we found that α is proportional to the length of the Ta absorber, which is consistent with the uniform quasiparticle loss.

The diffusion constant can be derived from the delay time of the two pulses from the tunnel junctions at each end of the absorber at a certain current threshold. The diffusion constant is calculated by fitting the experimental results with our numerical models. We find a diffusion constant $D = 8.2 \pm 0.2 \text{ cm}^2/\text{s}$ for the two devices. With the diffusion constant and loss parameter α we can calculate the quasiparticle lifetime in the Ta absorber $\tau_{Ta} = 83 \pm 5 \mu\text{s}$. The quasiparticle lifetime in the Nb contact region τ_{Nb} is $20 \pm 4 \mu\text{s}$. Another device with a 200 μm long Ta absorber has also been measured. It shows the same results, but it is too short to precisely determine the loss parameters. The fit of Q_1 vs. Q_2 of the device with the 500 μm long absorber is shown in Fig. 4. The region shown is part of that shown in Fig. 2. The black dots are the experimental events. The dashed line is the fit to the MnK_α events with only Ta loss. The solid line is the fit with Nb loss added. We see that the fit is slightly improved by inclusion of loss in the Nb overlap region, but the dominant loss mechanism is in the Ta film itself. The detailed fitting

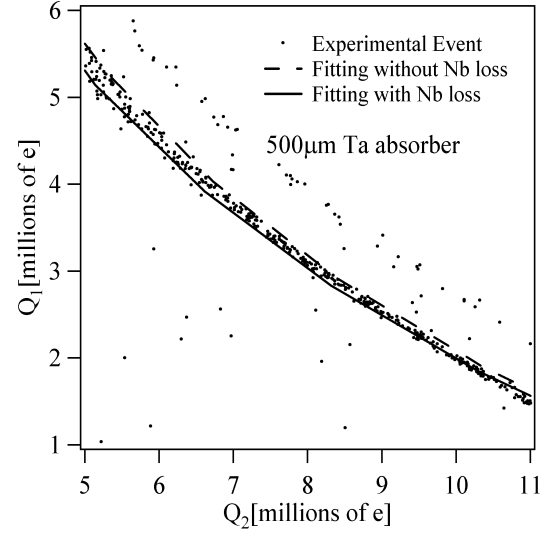


Fig. 4. Q_1 vs. Q_2 of two devices with different lengths. The dots are experimental x-ray events and the curve is from the fitting model with (solid line) and without Nb loss (dash line).

procedures are discussed in [11]. The substrate events and the photon events in the Ta-Al overlap region are eliminated from the fits in Fig. 4.

V. CONCLUSIONS

We measured two devices with different absorber lengths, 500 μm and 1000 μm . By fitting the experimental current pulses and charges with our model, we demonstrate that the dominant quasiparticle loss is that of the Ta absorber. The quasiparticle loss caused by the Nb contact is small compared to the uniform loss in the Ta. But the Nb contact adds extra broadening of the energy resolution in the center of the Ta absorber [8] because the Nb contacts only one side of the absorber. From the simulations, we calculate the quasiparticle diffusion constant $D = 8.2 \pm 0.2 \text{ cm}^2/\text{s}$, the quasiparticle lifetime in the Ta absorber $\tau_{Ta} = 83 \pm 5 \mu\text{s}$ and the quasiparticle loss time in the Nb contact region $\tau_{Nb} = 20 \pm 4 \mu\text{s}$. (Quasiparticles spend less time in that region as they diffuse in the Ta). The quasiparticle loss length, $(D\tau_{Ta})^{1/2} = 260 \mu\text{m}$, sets the scale for the length of the Ta film absorber fabricated with our present methods to be less than 1 mm. However, the measured diffusion constant is much smaller than the theoretical prediction of $27 \text{ cm}^2/\text{s}$ and the quasiparticle lifetime is much shorter than the theoretical value of 1 ms. There is not yet a microscopic explanation of these differences. If the experimental parameter values can be increased, much larger absorbers would be feasible. More discussion of this can be found in [12]. The diffusion constant, and possibly the loss time, might be improved by using a higher quality Ta film, such as a Ta epitaxial film. Our films are polycrystalline, as they are grown on a non-lattice-matched substrate, SiO_2 on Si. The epitaxial films studied at ESA are thinner than ours, and have $D=17 \text{ cm}^2/\text{s}$, $\text{RRR}=45$ and $\tau_{Ta} = 52 \mu\text{s}$ [13]. Thicker epitaxial films may give larger values of D and the loss time.

REFERENCES

- [1] N. Booth and D.J. Goldie, "Superconducting particle detectors", *Supercond. Sci. Technol.*, vol. 9, pp.493-516, 1996.
- [2] H. Kraus et al., "Quasiparticle trapping in a superconductive detector system exhibiting high energy and position resolution", *Phys. Lett. B*, vol. 231, pp.195-202, 1989.
- [3] S. Friedrich et al., "Experimental quasiparticle dynamics in a superconducting imaging x-ray spectrometer" *Appl. Phys. Lett.*, vol. 71, pp.3901-3903, 1997.
- [4] P.Verhoeve, N. Rando, A. Peacock, A. van Dordrecht, B.G. Taylor , and D.J.Goldie, "High-resolution x-ray spectra measured using tantalum superconducting tunnel junctions ", *Appl. Phys. Lett.*, vol. 72, pp.3359-3361, 1998;
- [5] G. Angloher, P. Hettl, M. Huber, J. Jochum, F. v. Feilitzsch and R.L. Mossbauer, "Energy resolution of 12 eV at 5.9 keV from Al-superconducting tunnel junction detectors", *J. Appl. Phys.* vol. 89, pp.1425-1429, 2001.
- [6] L. Li, et al., "X-ray single photon 1-D imaging spectrometers", *IEEE Tran. Appl. Supercond.* vol.11, pp. 685-688, 2001.
- [7] Fano factor for Sn: M. Kurakado, "Possibility of high resolution detectors using superconducting tunnel junctions", *Nucl. Instrun. Methods* 196, pp. 275-277, 1982; We assume Ta to be similar to Nb.
- [8] L. Li, et al., "Improved energy resolution of single photon imaging spectrometers using superconducting tunnel junctions", *J. Appl. Phys.* vol. 90, pp.3645-3647, 2001.
- [9] S. Friedrich, et al., "Single photon imaging x-ray spectrometers using low noise current preamplifiers with dc voltage bias", *IEEE Trans. Appl. Supercond.*, vol. 3, pp. 3383-3386, 1997.
- [10] K. Segall, Ph.D. Thesis, Yale University, 2000.
- [11] L. Li, Ph.D. Thesis, Yale University, 2002.
- [12] L. Li, L. Frunzio, C.M. Wilson and D.E. Prober, *J. Appl. Phys.* to be published, Feb. 2003.
- [13] R. den Hartog, et al., "Large-Format distributed read-out imaging devices for x-ray imaging spectroscopy", Ninth international workshop on low temperature detectors, F. S. Porter, et al. Ed., Wisconsin, pp.11-14, 2002.